Journal of Zhejiang University SCIENCE A
ISSN 1673-565X (Print); ISSN 1862-1775 (Online)
www.zju.edu.cn/jzus; www.springerlink.com
E-mail: jzus@zju.edu.cn

Study on inverter fault-tolerant operation of PMSM DTC*

Yznaga Blanco IVONNE[1,2], Dan SUN[†‡1], Yi-kang HE[1]

([1]*School of Electrical Engineering, Zhejiang University, Hangzhou 310027, China*)

([2]*Researches and Electrical Tests Center, Cujae University, Havana City 19390, Cuba*)

[†]E-mail: sundan@zju.edu.cn

Received July 23, 2007; revision accepted Oct. 30, 2007

Abstract: This paper presents an investigation of inverter fault-tolerant operation for a permanent magnet synchronous motor (PMSM) direct torque control (DTC) system under various inverter faults. The performance of a faulty standard 6-switch inverter driven PMSM DTC system is analyzed. To avoid the loss or even disaster caused by the inverter faults, a topology-modified inverter with fault-tolerant capability is introduced, which is reconfigured as a 3-phase 4-switch inverter. The modeling of the 4-switch inverter is then analyzed and a novel DTC strategy with a unique nonlinear perpendicular flux observer and feedback compensation scheme is proposed for obtaining a continuous, disturbance-free drive system. The simulation and experimental results demonstrate that the proposed inverter fault-tolerant PMSM DTC system is able to operate stably and continuously with acceptable static and pretty good dynamic performance.

Key words: Permanent magnet synchronous motor (PMSM), Direct torque control (DTC), Fault-tolerant operation, Four-switch inverter, Nonlinear perpendicular flux observer

doi:10.1631/jzus.A071399 **Document code:** A **CLC number:** TM302; TM351

INTRODUCTION

The permanent magnet synchronous motor (PMSM) direct torque control (DTC) system has attracted much attention at present because of its outstanding advantages, such as high torque/current ratio, high power density, high efficiency, high power factor, simplicity, robustness and excellent dynamic performance, compared with other types of motor drives (Takahashi and Ohmori, 1989; Zhong and Rahman, 1997). It is considered as one of the greatest potential to be adopted in automotive industries, electric vehicle, ship propulsion and other critical military situations (Diamantis and Prousalidis, 2004; Xing *et al*., 2005). The practical application of this technology, however, relies highly on its capability of maintaining continuous trouble-free operation and system reliability.

A modern electrical drive system generally consists of a power electronic inverter, a microprocessor controller and a motor. Depending on the control strategy, various sensors are employed to acquire essential information of the system status. According to the instruction signal and system status, the control algorithm stored in the microprocessor controller generates appropriate gate drive signals, which control the inverter to produce appropriate voltage space vectors to drive the motor with desired performance. In such a system, the inverter is a key component since any fault occurred without a pre-programmed fault-tolerant control strategy will cease the drive system, which may lead to disastrous economical loss. However, this can be avoided by incorporating a fault-tolerant control algorithm, which is able to maintain the system stable and generate a system fault signal to warn the system operator to clarify the problem.

In the past few years, a great amount of works have been conducted on the faults diagnosis and their

‡ Corresponding author

* Project supported by the National Natural Science Foundation of China (No. 50507017) and the SRF for ROCS, SEM

tolerant methods for motors (Cruz and Cardoso, 2004; Bellini *et al*., 2007; Lee and Habetler, 2007), inverters (Fu and Lipo, 1993; Kastha and Bose, 1994; Mendes and Marques Cardoso, 1998; 2003; Welchko *et al*., 2004; Sun and He, 2005; Gamal *et al*., 2007), and sensors (Lee and Ryu, 2003). But most of the literature focused on the PWM control or vector control strategy for motor or sensor faults, only few mentioned the continuous operation of DTC drive under inverter faults, especially for PMSM. Mendes and Marques Cardoso (2003) proposed two fault-tolerant operations for induction motor drive, where the vector control and DTC strategies were simulated for the post-fault system, but they did not provide any discussion on the vector plane variation and the implementation of DTC strategy for the post-fault system. A modified DTC strategy for PMSM under inverter fault was discussed by Sun and He (2005), however, only simulated results included.

This paper presents a solution for the inverter fault-tolerant operation of a PMSM DTC, in which the inverter faults, the fault-tolerant inverter topology and the fault-tolerant DTC strategy were dealt as a unit to reconstruct a reliable high performance PMSM DTC system. The correctness and feasibility of the proposed fault-tolerant operation scheme are numerically simulated and experimentally validated by a prototype system.

EFFECT OF INVERTER FAULTS IN PMSM DTC

Fig.1 illustrates the block diagram of the PMSM DTC system fed by a standard 6-switch voltage source inverter, which is triggered by an external gate drive circuit. Any failure of either the power electronic switches or the gate drive circuits could cause various inverter faults. The frequently happened ones include the single switch open- or short-circuit fault and the single-phase open-circuit fault (Fu and Lipo, 1993; Welchko *et al*., 2004). In a standard inverter, the single switch open-circuit fault might be caused by a breakdown gate electrode of the device, an open gate circuit or the loss of drive signal. The single switch short-circuit fault might happen when the reverse device breaks down or the insulation is destructed. This is a very serious fault because it might lead to a direct short-circuit of the two switches in the same phase bridge-leg and, as a result, to produce a large short-circuited current possible to destroy other devices. When this type of fault occurs, the protection circuit of the inverter will automatically switch off another switch in the same inverter leg to ensure the safety of the whole system. A single-phase open-circuit fault can be caused by the faulty gate drive circuits or disordered drive signals. Generally speaking, for a standard 6-switch inverter fed PMSM drive system, all of the above mentioned faults could happen. It is usually presumed in the study that only one fault occurs at a time and the happened fault will not cause other succeeding faults.

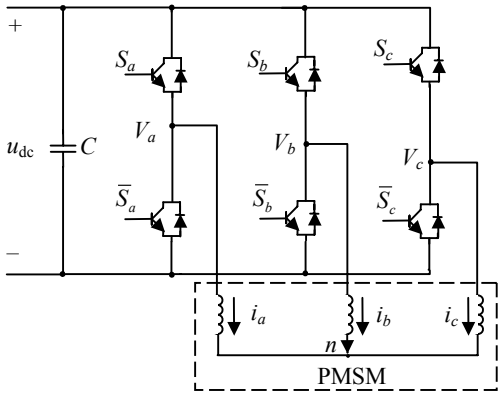

Fig.1 The standard 6-switch inverter fed permanent magnet synchronous motor (PMSM) drive system

The faulty condition of the system can usually be revealed by the deformed waveforms of phase current, voltage or flux linkage. However, Benbouzid and Kliman (2003) suggested that the phase current is the most appropriate quantity for the fault diagnosis. Fig.2 plots the simulated three-phase current waveforms from starting-up to steady state under both healthy and different faulty inverter conditions. As shown in Fig.2a, the three-phase current waveforms of the PMSM DTC drive fed by a healthy inverter are all sinusoidal after the system reaches the steady state. Figs.2b and 2c show the three-phase current waveforms when open-phase and open-switch faults occur, respectively, at t=0.1 s in Phase A, in which it is obvious that these waveforms are no longer sinusoidal. Fig.2d shows the phase current when a short-switch fault happened, which is a very serious fault for the inverter as the system cannot reach a steady state any longer. When this sort of fault occurs in one of the three legs, the terminal of motor phase winding is constantly connected to the DC bus through the short-circuited faulty switching device. To avoid the

short-circuit fault of the whole leg, the protection algorithm should switch off constantly the other switching device. Discussion of the specific fault diagnosis method based on the motor current is beyond the topic of this paper, which may be found in the related references (Mendes and Marques Cardoso, 1998; Peuget *et al*., 1998).

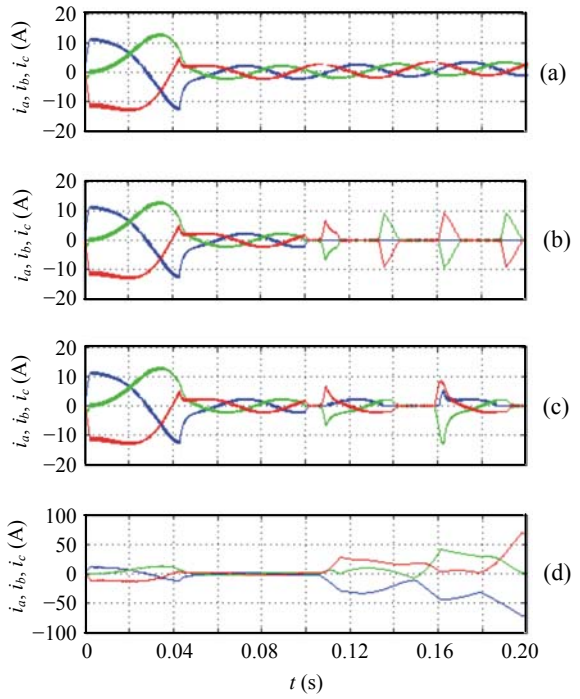

Fig.2 Phase currents of PMSM DTC drive under different operating conditions. (a) Healthy condition; (b) Open-phase fault occurs at t=0.1 s; (c) Open-switch fault occurs at t=0.1 s; (d) Short-switch fault occurs at t=0.1 s

It should be noted that when any of the above mentioned faults occurs, the drive system will cease its normal function and the protection measures provided by the system can only protect the system from further severer damage (Welchko *et al*., 2004). In order to minimize the economical loss caused by the drive system malfunction, it is greatly desired to develop a reliable fault-tolerant technique to maintain the basic drive performance until the fault cleared.

FAULT-TOLERANT INVERTER FED PMSM DTC

Fault-tolerant inverter

The standard 6-switch 3-phase inverter is not capable of maintaining the basic function of a drive system since it does not have the fault-tolerant capability. A few modified standard inverters for fault tolerance have been reported (Fu and Lipo, 1993; Welchko *et al*., 2004). Among them, a simplified switch-redundant type fault-tolerant inverter, as shown in Fig.3, is adopted in this paper for its features of simple circuit topology, low-cost, good compatibility and strong fault-tolerant capability.

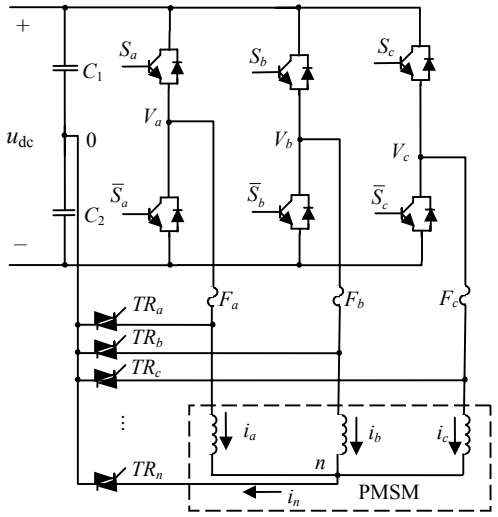

Fig.3 A simplified switch-redundant type fault-tolerant inverter

To form this fault-tolerant inverter, four extra TRIACs (TR_a, TR_b, TR_c, TR_n), one more capacitor and three fast acting fuses (F_a, F_b, F_c) are added to the standard 6-switch 3-phase inverter. In the normal operation condition, four TRIACs are switched off, which makes the inverter operate in exactly the same way as that of a standard inverter. When a short-/open-circuit fault or an open-phase fault in the leg of Phase A is sensed, for example, the control algorithm sends the gate driven signals out to turn on TRIAC TR_a and blow out fuse F_a in order to open-circuit the faulty leg, resulting in a post-fault topology with the Phase A terminal of the motor connected directly to the middle point of the DC bus capacitor, as shown in Fig.4, which is referred to as a 4-switch 3-phase inverter. It should be mentioned that this fault-tolerant topology is also capable of dealing with the motor side faults. When an open-/short-circuit fault in one of the motor windings is sensed, the control algorithm will check the gate drive signals to open the related bridge leg and turn on TRIAC TR_n, resulting in another 4-switch 2-phase inverter topology, which is not considered in this paper.

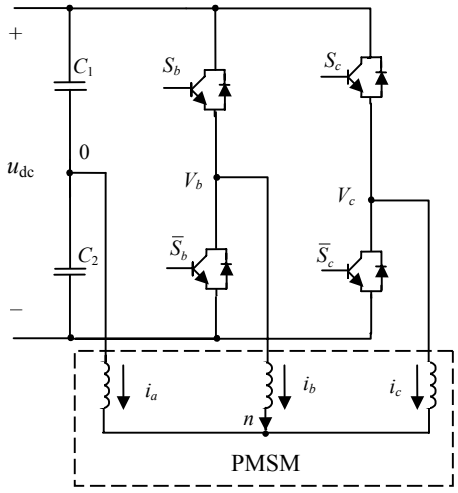

Fig.4 Post-fault 4-switch 3-phase inverter

Model of fault-tolerant inverter

In the 4-switch inverter, as shown in Fig.4, a three-phase system is obtained by connecting the Phase A terminal of the stator windings directly to the middle point of the DC bus capacitors, in which the stator current is exactly the same as that in a standard inverter fed system. The stator current vector is then formulated as

$$i_s=2(i_a+\alpha i_b+\alpha^2 i_c)/3, \tag{1}$$

and its α-β reference frame components are

$$\begin{cases} i_{s\alpha}=(2i_a-i_b-i_c)/3, \\ i_{s\beta}=\sqrt{3}(i_b-i_c)/3. \end{cases} \tag{2}$$

Since only two legs of the inverter are connected to the stator winding terminals B and C, the stator phase voltages are different from those of the standard inverter driven system. The stator voltage vector can be expressed in the same format as that in the standard inverter fed system as

$$u_s=2(u_{an}+\alpha i_{bn}+\alpha^2 u_{cn})/3. \tag{3}$$

Its *a*-*b*-*c* reference frame components are expressed as

$$\begin{cases} u_{an}=u_{dc}(1-S_b-S_c)/3, \\ u_{bn}=u_{dc}(2S_b-S_c-0.5)/3, \\ u_{cn}=u_{dc}(2S_c-S_b-0.5)/3, \end{cases} \tag{4}$$

and the α-β reference frame components are

$$\begin{cases} u_{s\alpha}=u_{dc}(1-S_b-S_c)/3, \\ u_{s\beta}=u_{dc}\sqrt{3}(S_b-S_c)/3, \end{cases} \tag{5}$$

where $\alpha=e^{j2\pi/3}$, u_{dc} is the DC bus voltage, S_b and S_c represent the switching states (0 or 1) of upper switches in the legs of Phases B and C, respectively.

Voltage vectors and system rating

According to Eq.(5), the voltage vector plane in the α-β reference frame of the 4-switch inverter driven system can be drawn as Fig.5, where $\boldsymbol{V}_1$, $\boldsymbol{V}_2$, $\boldsymbol{V}_3$ and $\boldsymbol{V}_4$ are the four voltage vectors generated by the inverter, (00), (10), (11) and (01) denote the switching states of S_b and S_c, respectively, and S1~S4 are the four sectors divided directly by the four voltage vectors.

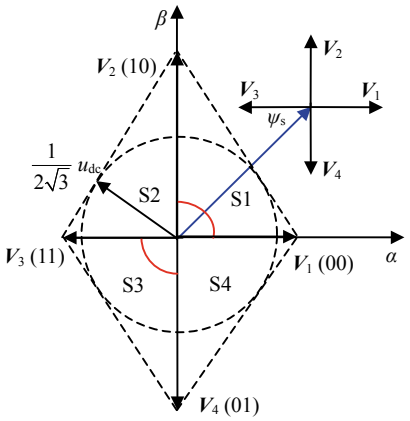

Fig.5 Voltage vector plane of a 4-switch inverter fed system

As shown in Fig.5, there exist only four symmetric active vectors with unequal amplitudes and no null voltage vector any more. It can also be seen that the 4-switch inverter is only capable of producing a fundamental phase voltage with peak amplitude of $u_{dc}/(2\sqrt{3})$ under optimal PWM control without over-modulation, which is only half of $u_{dc}/\sqrt{3}$ for a standard 6-switch inverter under normal operation condition. However, the 4-switch inverter is capable of producing a full rated current, being the same as the standard healthy inverter. As far as the motor capacity is concerned, this 4-switch topology could allow the motor producing the rated torque, which will make the system enter in field weakening operation mode at approximately half of the rated speed.

Voltage vector switching table of the 4-switch inverter fed DTC system

The block diagram of a PMSM DTC system with the fault-tolerant inverter is shown in Fig.6.

The system basically comprises two hysteresis controllers, flux linkage and torque calculator, voltage vector switching table, inverter, the relevant control circuit for the fault diagnosis and fault isolation and PMSM. Here, the switching table should be correspondingly rearranged according to the new voltage vectors when the fault-tolerant 4-switch inverter is reconfigured after fault occurrence. The effect of different voltage vectors can be explained as follows: if the present stator flux linkage vector $\boldsymbol{\psi}_s$ stands in section S1, the applying of voltage vector $\boldsymbol{V}_1$ will increase the flux linkage amplitude and decrease the torque, whereas $\boldsymbol{V}_2$ increases the flux linkage amplitude and increases the torque. Following the same principle, a voltage vector switching table for the 4-switch inverter fed DTC system can be tabulated in Table 1.

Table 1 Voltage vector switching table

Flux	Torque	S1	S2	S3	S4
0	0	$\boldsymbol{V}_4$	$\boldsymbol{V}_1$	$\boldsymbol{V}_2$	$\boldsymbol{V}_3$
0	1	$\boldsymbol{V}_3$	$\boldsymbol{V}_4$	$\boldsymbol{V}_1$	$\boldsymbol{V}_2$
1	0	$\boldsymbol{V}_1$	$\boldsymbol{V}_2$	$\boldsymbol{V}_3$	$\boldsymbol{V}_4$
1	1	$\boldsymbol{V}_2$	$\boldsymbol{V}_3$	$\boldsymbol{V}_4$	$\boldsymbol{V}_1$

'Flux' and 'Torque' are the logic variables denoting the need of flux linkage and torque, respectively, in which '0' means needed to decrease and '1' means needed to increase

NUMERICAL SIMULATION

Based on Fig.6, the fault-tolerant inverter fed PMSM DTC system has been simulated under both healthy and faulty conditions by using MATLAB/SIMULINK. The parameters of the motor are shown in Table 2.

Table 2 Motor parameters

Parameter	Value
Number of pole pairs P_n	3
Stator resistance R_s	0.56 Ω
Permanent magnet flux linkage ψ_r	0.1663 Wb
Rated voltage u_N	128 V
Rated current I_N	15.8 A
d-q inductance L_d, L_q	15.3 mH
Rated speed ω_N	2000 r/min

Fig.7 shows the simulated system performance in which the PMSM was fed by the fault-tolerant 6-switch inverter using the basic DTC strategy initially. A sudden inverter fault was assumed to occur in Phase A at t=0.2 s and then a 4-switch 3-phase inverter is reconfigured and controlled immediately with the modified DTC scheme. In order to maintain a circular flux linkage trajectory and considering the system rating of the 4-switch inverter system simultaneously, the reference speed is set at half the rated speed (1000 r/min) to insure the disturbance-free operation. The speed, torque, flux linkage, phase voltage u_{ab} and current i_a, i_b and i_c waveforms of the

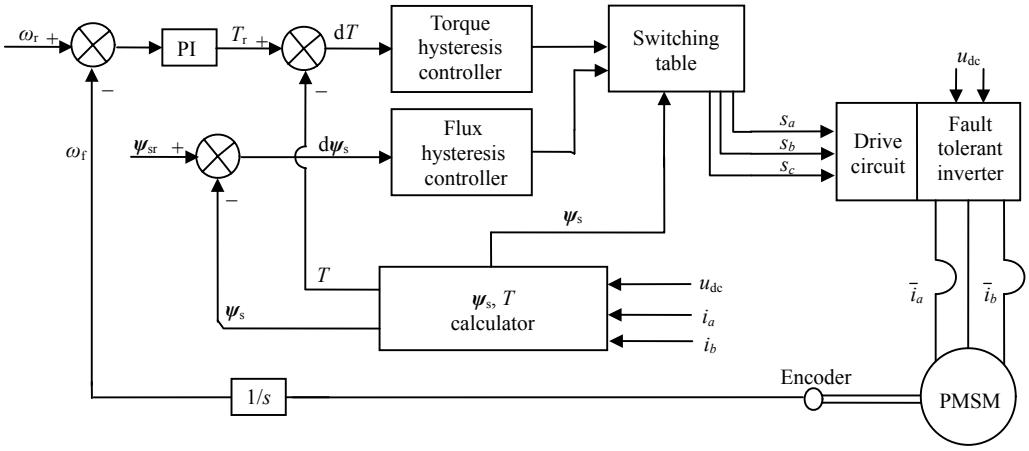

Fig.6 Block diagram of the fault-tolerant inverter fed PMSM DTC

system from the healthy to faulty conditions are all shown in Fig.7 from top to bottom, respectively. It can be seen from the figures that the system is capable of operating continuously and steadily after the fault occurrence but with u_{ab} changed to be half of the u_{dc} and the ripples of torque, flux linkage and currents being all larger with higher frequency under the fault condition. Figs.8a and 8b show the trajectories of the stator flux linkage before and after the fault occurrence, respectively. As shown, these two flux linkage trajectories are different to some extent due to the different voltage vectors applied although both of them are circular.

The second numerical test is conducted to examine the post-fault starting-up capability of the proposed system. The starting-up performance of the system fed by the 4-switch 3-phase inverter is plotted in Fig.9 with the speed, torque, flux linkage, line to line voltage u_{ab} and the three-phase currents i_a, i_b and i_c waveforms shown from top to bottom, respectively. It can be seen that the post-fault system can still operate steadily with acceptable performance.

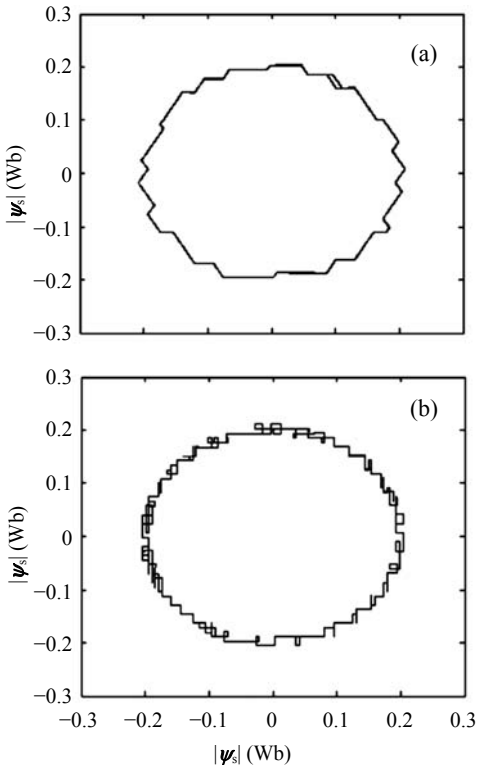

Fig.8 Stator flux linkage locus before fault (a) and after fault (b)

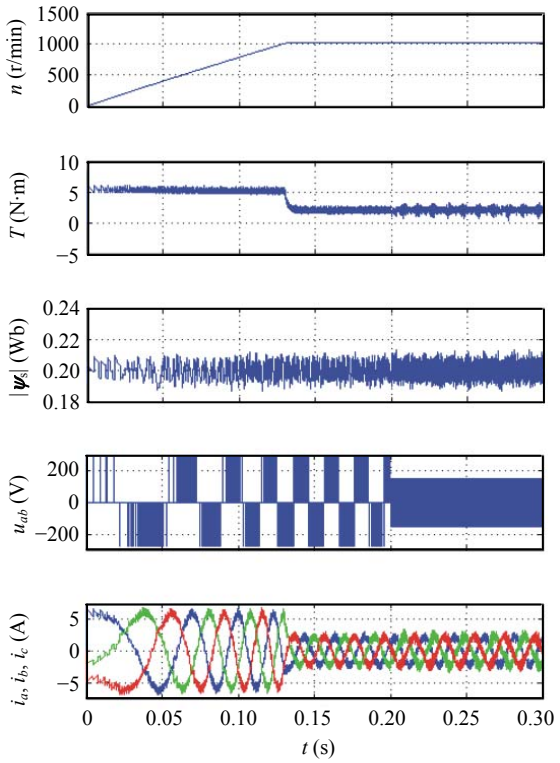

Fig.7 Transient performance of the fault-tolerant PMSM DTC system

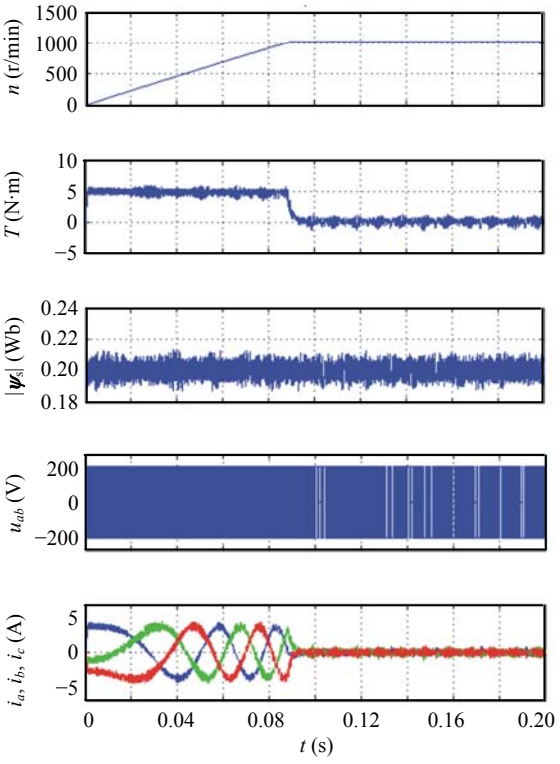

Fig.9 Starting-up performance of the post-fault inverter fed PMSM DTC drive system

EXPERIMENTAL VERIFICATION

To make deep experimental investigation, a hardware setup, including a digitally controlled IGBT based fault-tolerant voltage source inverter and a TI TMS320C240 DSP controller, was built up. The PMSM under test is coupled to a separately excited DC machine via a torque-meter. All the parameters used are the same as those in the simulation study.

It is well known that the low speed performance of a practical DTC drive system is usually not very good mostly because of the estimation error of flux linkage at low speed. This problem is even more serious in the 4-switch inverter fed DTC system since only four uneven-amplitude voltage vectors are available, which sometimes worsens the correctness of flux observation in the starting-up process for an experimental system. To solve this problem, a nonlinear perpendicular flux observer with feedback compensation, as discussed by Jia and He (2005), is necessary to be adopted.

Fig.10 shows the schematic diagram of the nonlinear perpendicular flux observer, served to ensure the stator flux observation correct and precise in a PMSM DTC system. As well-known, the motor stator flux is the integration of its back electromotive force (EMF) ***emf***, i.e.,

$$\boldsymbol{\psi}_s = \int_0^t (\boldsymbol{u}_s - R_s \boldsymbol{i}_s)\mathrm{d}t + \boldsymbol{\psi}_s(0), \tag{6}$$

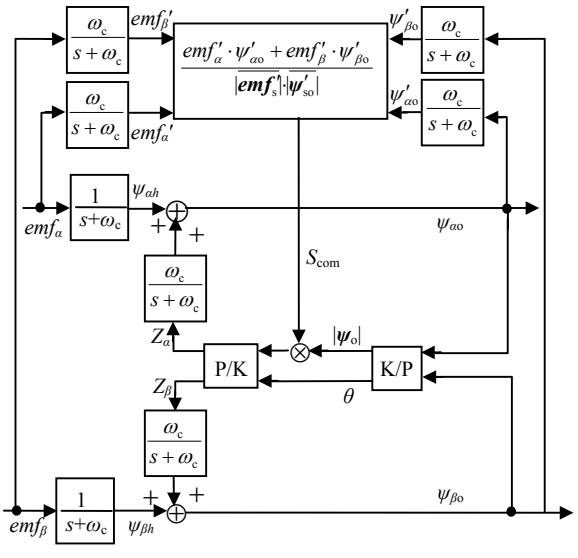

Fig.10 Nonlinear perpendicular flux observer

where $\boldsymbol{u}_s$, $\boldsymbol{i}_s$, $\boldsymbol{\psi}_s$, $\boldsymbol{\psi}_s(0)$ are the stator voltage vector, current vector, stator flux vector and the initial stator flux vector established by rotor permanent magnets, respectively. The term $(\boldsymbol{u}_s - R_s\boldsymbol{i}_s)$ is certainly the back EMF, which, as a vector, should be perpendicular to the stator flux vector $\boldsymbol{\psi}_s$ if the flux observer operates correctly. However in the DTC system, to obtain a quickly dynamic torque response, quite different space voltage vectors are applied during two successive control periods in order to drive the stator flux vector changing quickly, which causes that the applied stator voltage vectors, $\boldsymbol{u}_s$, are discrete. Due to the existence of stator winding inductances, the stator currents can still be kept as continuous quantities and, naturally, the voltage drop across the stator resistance $R_s\boldsymbol{i}_s$ is continuous as well, which leads to a non-continuous back EMF $(\boldsymbol{u}_s - R_s\boldsymbol{i}_s)$ and makes the conventional flux observation via back EMF no longer accurate enough for the DTC application, especially at the low speed.

In Fig.10, the back EMF vector ($\boldsymbol{emf}_s$) has been decomposed into two components of emf_α and emf_β in the α-β reference frame. To make the $\boldsymbol{emf}_s$ continuous, a low-pass filter $1/(s+\omega_c)$ is set behind both emf_α and emf_β, which makes these two components become emf_α' and emf_β', and naturally causes a certain phase shift for $\boldsymbol{emf}_s'$.

On the other hand, the correctness and accuracy of flux observing can be judged by the perpendicularity of the EMF vector to the flux vector. According to (Jia and He, 2005), the flux estimation algorithm suitable for PMSM DTC application can be formulated as

$$\boldsymbol{\psi}_{so} = \frac{\boldsymbol{emf}_s}{s+\omega_c} + \frac{\omega_c}{s+\omega_c} S_{com}\boldsymbol{\psi}_{so}, \tag{7}$$

where S_{com} is the flux compensation coefficient, determined by the perpendicular degree of the stator flux vector $\boldsymbol{\psi}_{so}$ to the back EMF vector $\boldsymbol{emf}_s$, and can be further expressed as

$$S_{com} = \frac{emf_\alpha'\psi_{\alpha o}' + emf_\beta'\psi_{\beta o}'}{|\boldsymbol{emf}_s'||\boldsymbol{\psi}_{so}'|}, \tag{8}$$

where $\psi_{\alpha o}'$ and $\psi_{\beta o}'$ are the two components of $\boldsymbol{\psi}_{so}$ after passing the same low-pass filter $1/(s+\omega_c)$ in order to make $\boldsymbol{\psi}_{so}'$ have an identical phase shift as that for $\boldsymbol{emf}_s$.

If the flux observed is perpendicular to the back EMF, the angle θ between them should be 90° and accordingly the cosine value of θ should be zero, which makes S_{com}=0, Z_α=0 and Z_β=0 in Fig.10, and means that no compensation flux is required and the flux has been estimated accurately. Otherwise, $\theta \neq 90°$ and $S_{com} \neq 0$, $Z_\alpha \neq 0$ and $Z_\beta \neq 0$, which indicate that the flux is not estimated accurately and the flux compensation measure must be adopted. As a result, the application of nonlinear perpendicular flux observer is capable of ensuring the stator flux observed accurately over a wide speed range, which effectively guarantees the successful starting-up for the 4-switch inverter fed PMSM DTC drive system.

Experimental operations have been conducted to test the performance of the post-fault PMSM DTC system, which is illustrated in Fig.11. Fig.11a shows the starting-up performance with speed and torque recorded for the post-fault 4-switch inverter fed system at the reference speed of 1000 r/min with very light load. These results demonstrate that the system is capable of starting-up smoothly with acceptable steady state and dynamic performance after employing the nonlinear perpendicular flux observer. Fig.11b shows the stator flux linkages components in the α-β reference frame, and Fig.11c shows the flux locus in the steady state, which is a round trajectory thanks to the correct estimation by the new flux observer. Fig.11d shows the phase currents i_a and i_b at no load, where both of them are almost zero. Fig.11e shows the torque response under a step-change of reference torque from zero to 2 N·m when the system operates with opened speed-loop. The response time is approximately 1.8 ms, which means that the post-fault PMSM DTC system still has pretty good dynamic performance.

CONCLUSION

Direct torque control (DTC) is a kind of high-performance control strategies, which is normally implemented in a 6-switch three-phase inverter. But in the converter fault condition, a 4-switch inverter becomes a replacing solution for keeping the system operating uninterrupted. The 4-switch inverter fed DTC system performance at low speed is not good enough since only four uneven-amplitude voltage vectors are available, which sometimes worsens the correctness of flux observation in the starting-up process for a practical system. A new nonlinear perpendicular flux observer with feedback compensation is an effective technical measure, which is capable of ensuring the stator flux observed accurately over a

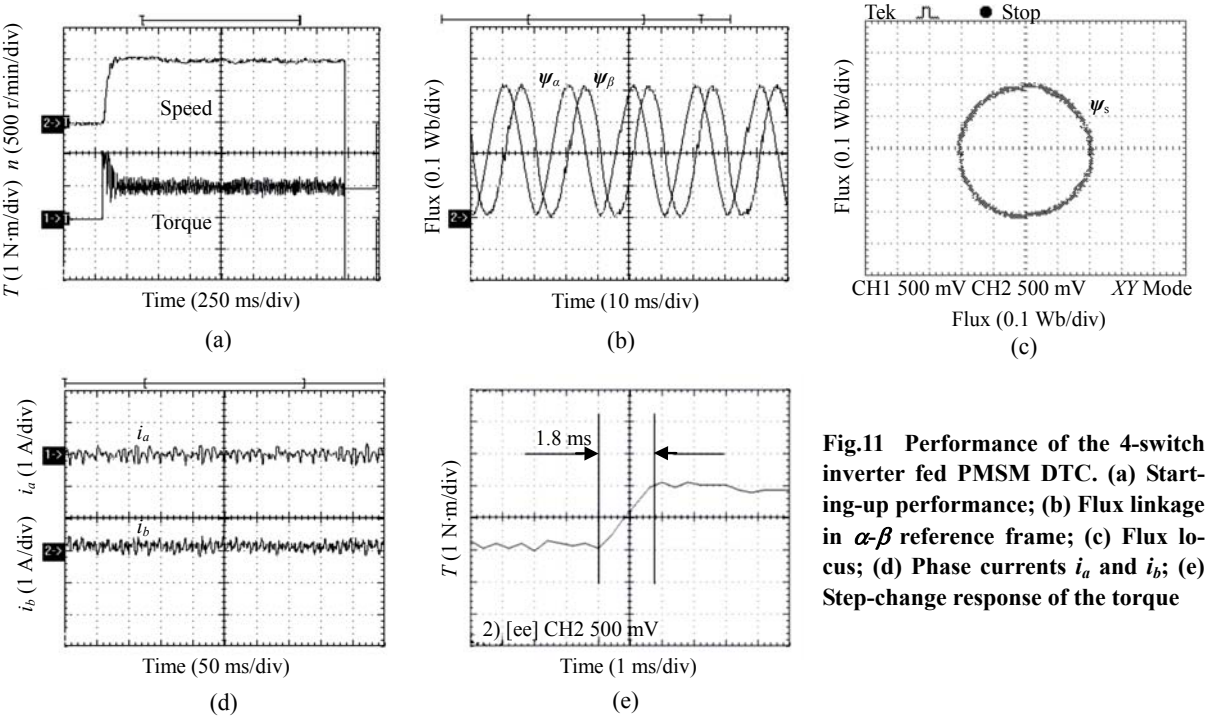

Fig.11 Performance of the 4-switch inverter fed PMSM DTC. (a) Starting-up performance; (b) Flux linkage in α-β reference frame; (c) Flux locus; (d) Phase currents i_a and i_b; (e) Step-change response of the torque

wide speed range and guaranteeing successful operation at low speed and starting-up for the 4-switch inverter fed PMSM DTC drive system. Detailed simulation and experimental tests verify that with the proposed fault-tolerant scheme and the novel nonlinear perpendicular flux observer, the PMSM DTC drive system is able to maintain its stable operation with a slightly degraded performance, which can effectively minimize the economical loss caused by cease of some function of the drive system during some operation failures.

References

Bellini, A., Concari, C., Franceschini, G., Tassoni, C., 2007. Different Procedures for the Diagnosis of Rotor Fault in Closed Loop Induction Motors Drives. Int. IEEE Electric Machines and Drives Conf., **2**:1427-1433. [doi:10.1109/IEMDC.2007.383638]

Benbouzid, M.E.H., Kliman, G.B., 2003. What stator current processing-based technique to use for induction motor rotor faults diagnosis? *IEEE Trans. on Energy Conv.*, **18**(2):238-244. [doi:10.1109/TEC.2003.811741]

Cruz, S.M.A., Cardoso, A.J.M., 2004. Diagnosis of stator inter-turn short circuits in DTC induction motor drives. *IEEE Trans. on Ind. Appl.*, **40**(5):1349-1360. [doi:10.1109/TIA.2004.834012]

Diamantis, G., Prousalidis, J.M., 2004. Simulation of a Ship Propulsion System with DTC Driving Scheme. Proc. 2nd Int. Conf. on Power Electronics, Machines and Drives, **2**:562-567.

Fu, J.R., Lipo, T.A., 1993. A Strategy to Isolate the Switching Device Fault of a Current Regulated Motor Drive. IEEE Industry Applications Society Annual Meeting, **2**:1015-1020.

Gamal, M., Mahmoud, M., Ibrahim, E.A., 2007. Inverter Faults in Variable Voltage Variable Frequency Induction Motor Drive. Compatibility in Power Electronics. Gdansk, Poland, p.1-6.

Jia, H.P., He, Y.K., 2005. Study on a New Nonlinear Perpendicular Flux Observer with Feedback Compensation for DTC Application. Proc. Eighth Int. Conf. on Electrical Machines and Systems. Nanjing, China, **3**:1824-1827.

Kastha, D., Bose, B.K., 1994. Investigation of fault modes of voltage-fed inverter system for induction motor drive. *IEEE Trans. on Ind. Appl.*, **30**(4):1028-1038. [doi:10.1109/28.297920]

Lee, K.S., Ryu, J.S., 2003. Instrument fault detection and compensation scheme for direct torque controlled induction motor drives. *IEE Proc.-Control Theory & Appl.*, **150**(4):376-382. [doi:10.1049/ip-cta:20030596]

Lee, Y.K., Habetler, T.G., 2007. An On-line Stator Turn Fault Detection Method for Interior PM Synchronous Motor Drives. Proc. 22nd Annual IEEE Applied Power Electronics Conf. CA, USA, p.825-831.

Mendes, A.M.S., Marques Cardoso, A.J., 1998. Voltage Source Inverter Fault Diagnosis in Variable Speed AC Drives, by the Average Current Park's Vector Approach. IEE Seventh Int. Conf. on Power Electronics and Variable Speed Drives, p.704-706.

Mendes, A.M.S., Marques Cardoso, A.J., 2003. Continuous Operation Performance of Faulty Induction Motor Drives. IEEE Int. Conf. on Electric Machines and Drives, p.547-553.

Peuget, R., Courtine, S., Rognon, J.P., 1998. Fault detection and isolation on a PWM inverter by knowledge-based model. *IEEE Trans. on Ind. Appl.*, **34**(6):1318-1326. [doi:10.1109/28.739017]

Sun, D., He, Y.K., 2005. A Modified Direct Torque Control for PMSM Under Inverter Fault. Proc. Eighth Int. Conf. on Electrical Machines and Systems, **3**:2469-2473.

Takahashi, I., Ohmori, Y., 1989. High-performance direct torque control of an induction motor. *IEEE Trans. on Ind. Appl.*, **25**(2):257-264. [doi:10.1109/28.25540]

Welchko, B.A., Lipo, T.A., Jahns, T.M., Schulz, S.E., 2004. Fault-tolerant three-phase AC motor drive topologies: a comparison of features, cost, and limitations. *IEEE Trans. on Power Electr.*, **19**(4):1108-1116. [doi:10.1109/TPEL.2004.830074]

Xing, W., Zhu, J.G., Xu, J.Q., Tang, R.Y., 2005. Design of a drive system based on TMS320LF2407 in EV application. *J. Shenyang Univ. Tech.*, **27**(1):23-27.

Zhong, L., Rahman, F., 1997. Analysis of direct torque control in permanent magnet synchronous motor drives. *IEEE Trans. on Power Electr.*, **12**(3):528-536. [doi:10.1109/63.575680]